3rd URSI AT-AP-RASC, Gran Canaria, 29 May – 3 June 2022

Look Up and Around: Accurate Precipitation Estimation by Merging Satellite Communication Data and Radar Measurements

Julian Krebs*[(1)(2)], Ahmad Gharanjik[(2)], M. R. Bhavani Shankar[(1)] and Kumar Vijay Mishra[(1)(3)]
(1) Interdisciplinary Centre for Security, Reliability and Trust (SnT),
University of Luxembourg, Luxembourg City L-1855, Luxembourg
(2) Databourg Systems S.A R.L-S, Luxembourg City L-1911 Luxembourg
(3) United States CCDC Army Research Laboratory, Adelphi, MD 20783 USA

Abstract

Accurate rain measurements with a high resolution in real-time are required for many applications such as extreme weather event prediction and protection of human life. Given two very different rain estimation techniques, the idea of this paper is to improve the rain accuracy by combining both methods to balance out each others disadvantages. To this end, a novel machine learning algorithm for retrieving rain rate from communication satellite signals and combining its estimates with state-of-the-art weather radar data is proposed. The preliminary results show that using a linear combination of both signals outperforms either of the methods independently when compared to the ground-truth measurements. In addition, the higher temporal resolution of the satellite signals in contrast to radar data is maintained for the combined rain estimation.

1 Introduction

Many applications including weather forecast, flood monitoring and the prediction of natural hazards such as the recent extreme weather events around the world require accurate precipitation estimates in real-time. The insurance, agriculture, traffic and transportation businesses rely on accurate weather data to avoid financial losses, accidents and secure human life. Being the state-of-the-art, weather radars are able to monitor the spatio-temporal dynamics of precipitation. However, they have their own limitations in terms of costs, accuracy and resolution. Due to their location on the ground and their horizontal observation of the surrounding, weather radars may additionally suffer from inaccurate results. For example, in mountainous regions radar beams are blocked by high-level terrain and low-level precipitation (in valleys) are missed [1].

Complementing this approach, existing user terminals used in satellite communication services (e.g. end-user broadband internet) have shown the potential to function as accurate local rain sensors [2, 3, 4, 5]. Here, the rain-induced signal attenuation is estimated by analyzing the regularly collected carrier-to-noise (C/N) signal between the satellite and user ground terminal (forward link). The relationship between the attenuation and rain rate at millimeter-wave then allows the computation of the latter. This relationship can be defined explicitly using the ITU-R power-law [6] which however, requires the attenuation induced by rain and not other factors. To tackle this difficulty of detecting rain events and rain-induced attenuation accurately, machine learning approaches are often used to learn from measurements of co-located rain gauges. These methods utilize dense [4] or long short-term memory networks [5] taking a temporal sequence of C/N values from one terminal as input to obtain the local rain rate. Finally, given the local rain rates of all terminals in a region of interest, a two-dimensional (2-D) rain map can be created using interpolation techniques such as ordinary kriging [7].

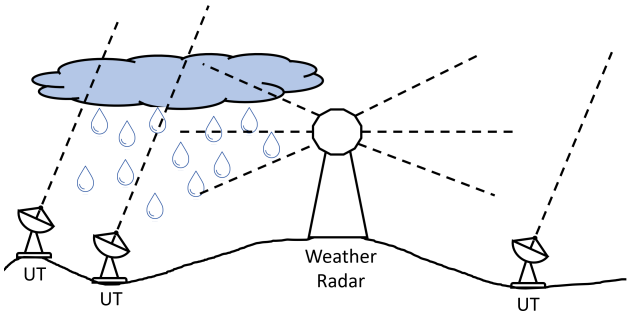

Figure 1. Combining satellite signals from user terminals (UT, used for broadband internet access) and weather radar data allows to measure rain more precisely by benefiting from the different estimation techniques.

Using existing satellite communication infrastructure for rain monitoring, is very economic as no additional sensing hardware needs to be installed. In addition, ground terminals report C/N values with a high frequency and since they point towards space, the terrain limitations from weather radars are resolved. However, for the creation of highly reliable 2-D rain maps, a high number of ground terminals is required. Also, heavy rain events are sometimes not accurately measurable if the C/N signal falls below the minimum required value in which case terminal outages occur [2].

In this work, we propose a novel way of precipitation estimation by combining rain estimates from satellite communication and weather radar data as shown in Fig. 1. To this end, we retrieve high-dimensional rain maps from a large network of user terminals using convolutional neural networks (CNN) before linearly combining the two estimates in a point-wise fashion. The approach demonstrates state-of-the-art rain estimation results. The main contributions are:

- Large-scale rain estimation using satellite communication data based on convolutional neural networks.
- Improved precipitation estimation by combining the satellite rain data with weather radar estimates.
- State-of-the-art high-dimensional 2-D rain map generation in real-time.

2 Methods

The approach consists of two steps: First, rain intensities are estimated and rain maps are created using a large network of user terminals providing broadband internet via satellite. Second, we extrapolate the rain intensities from weather radars to fit the spatial grid and the higher temporal resolution of the satellite rain maps created in the first step. Finally, both rain estimates are combined.

2.1 Rain Map Generation via Satellite Communication Signals

In this work, the rain rate z_t at a user terminal for a given time t and temporal sequence of C/N values $\mathbf{x}_t$ with length T is estimated using two one-dimensional CNNs: one for classifying rain and dry events and one for obtaining the rain rate in case of a rain event. In a second step, the estimated rain rates from all user terminals are combined to generate 2-D rain maps.

The first CNN is a classification network f_y aiming at differentiating rainy and dry events at time t: $y_t = f_y(\mathbf{x}_t)$ with y_t being a binary decision of rain or dry. The sequence of C/N values $\mathbf{x}_t$ consists of the T most recent C/N values with the last one being at time t and which are collected every 5 minutes. In this work, we set $T = 24$ to consider the last two hours of data. The rain rate z_t is then obtained by:

$$z_t = \begin{cases} f_z(\mathbf{x}_t), & \text{if } y_t = 1 \\ 0, & \text{otherwise} \end{cases}, \tag{1}$$

where f_z is a second CNN that regresses the rain rate z_t directly from the sequence of C/N values $\mathbf{x}_t$.

During training with stochastic gradient decent, the parameters of the 2 CNNs are optimized in a supervised way using a binary cross-entropy function for the classification CNN and a mean-squared error function for the rain rate regression CNN. Here, measurements from rain gauges and weather radar are used as ground truth data.

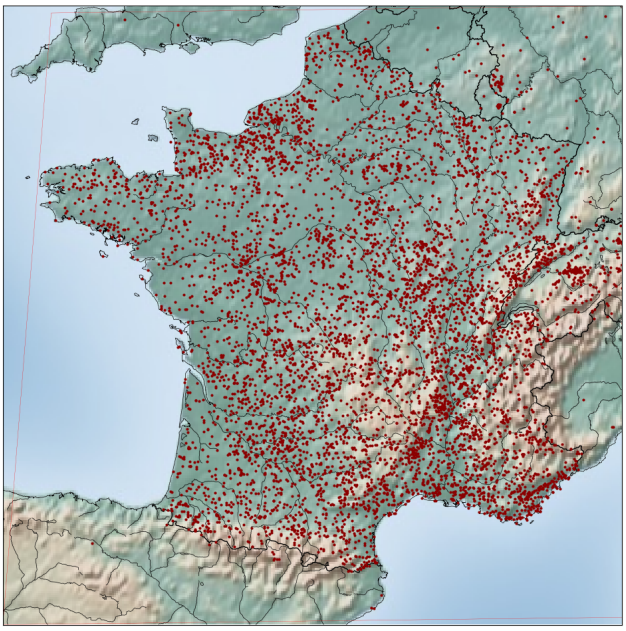

Figure 2. User terminals for broadband internet access in France.

After estimating the rain rates $\mathbf{z}$ from all user terminals, the results are used to generate 2-D rain maps $R^S \in M \times N$ where M and N are the sets of longitudes and latitudes. In this work, we apply ordinary kriging [7] using a power variogram model and a moving window approach to handle the high dimensionality of the rain maps. The results are rain rates $r_{ij} \quad \forall i \in \{1,\ldots,N\}, j \in \{1,\ldots,M\}$ on a regular 1×1 km grid.

2.2 Combining Satellite and Radar Rain Maps

Since the radar images are available every 15 minutes while the satellite based approach yields one every 5 minutes, the first step is to extrapolate the former to 5 min intervals. More precisely, the STEPS [8] nowcasting approach that uses optical flow with a probabilistic component is applied to generate radar images after 5 and after 10 minutes respectively given the 3 previous radar images. In addition, the radar data with a resolution of 2×2 km is linearly interpolated to fit the 1×1 km grid of satellite rain maps. The resulting 5 minute radar rain maps are denoted by $r^S_{ij} \quad \forall i \in \{1,\ldots,N\}, j \in \{1,\ldots,M\}$.

Finally, the two rain maps are combined per pixel using global weighting factors α and β (2) resulting in the combined rain rate r^C_{ij}.

$$r^C_{ij} = \alpha r^S_{ij} + \beta r_{ij} \quad \forall i \in \{1,\ldots,N\}, j \in \{1,\ldots,M\}. \tag{2}$$

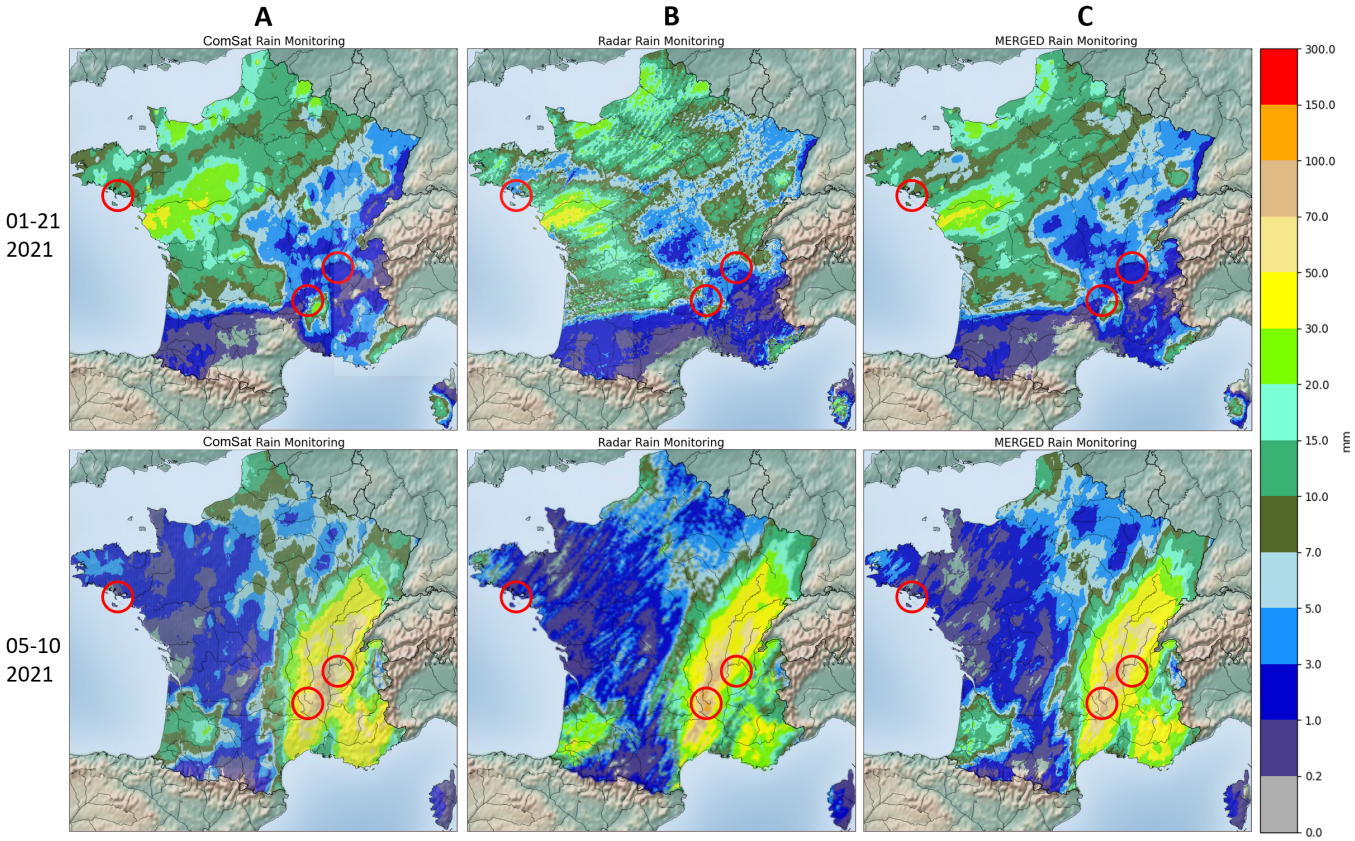

Figure 3. Rain accumulation (in mm) over 24 hours for two days in 2021 estimated using communication satellite signals (A, ComSat), weather radar data (B) and combining both (C).

The sum of α and β is 1 and thus, they reflect the confidence on each measurement and can be fixed or dynamic in time and per region. For this paper, α and β were chosen heuristically as 0.5 and fixed over all experiments.

3 Experiments

We evaluate our method on a network of 8.200 user terminals distributed in Metropolitan France with C/N data every 5 minutes. Their locations are shown in Fig.2. We used 110 additional terminals in France and Germany and 4 months of data (September-December 2020) for training our algorithm. As supervision, rain gauges from the German Weather Service [9] were used that had 5 minute resolution and were in close proximity (<5km) to 10 of the training terminals. For the remaining terminals, co-located weather radar data (OPERA [10], 15 minute resolution) were used as training supervision.

For the validation, we identified 37 days with rain events (between January 21 and July 5, 2021). We produced the rain maps using satellite data (5min, 1km^2), radar data [10] (15min, 2km^2) and the combination of both (5min, 1km^2). We collected data of 42 rain gauges in France [11] for these dates which we considered as ground-truth rain measurements at their locations. For comparing the different methods, we converted the rain rates to rain amount per day (mm per day). Thus, we computed the 24 hour rain accumulation. We then computed the error with respect to rain gauge measurements at their locations.

4 Results

In Table 1, the error statistics of the 24-hour accumulated rain of the different methods is shown at all 42 rain gauge locations and 37 days. The combined rain maps show an average error of 1.95mm per 24 hours, while radar and satellite (ComSat) estimation had an error of 2.29mm respectively 2.64mm. In the per-day competition between the three methods, the combined rain estimation shows the lowest average error among the 42 rain gauges in 21 out of 37 days.

Table 1. 24-hour rain error statistics with respect to rain gauge estimations at 42 locations over 37 days showing mean, median and standard deviation in mm and the number of days with lowest average error (of all rain gauges) among the three methods (Best). Comparing rain estimates from satellite signals (ComSat), radar and their combination.

Method	Mean	StDev	Median	Best
ComSat	2.64	4.37	1.00	3
Radar	2.29	4.00	0.71	13
Combined	**1.95**	**3.46**	**0.70**	**21**

The visualization of 24-hour rain accumulation in France of January 21 and May 10, 2021 for the three different methods is shown in Fig. 3. In addition, we report the 24-hour rain accumulation at three rain gauges in Frances for these two days in Table 2. The locations of Lyon, Belle Ile and Le Puy (marked in Fig. 3 are chosen for their significant location and rain intensity during the two days.

Table 2. 24-hour rain accumulation in mm at 3 rain gauge locations comparing radar, satellite and combined methods. In bold the closest rain measurements to rain gauge (ground truth).

	Gauge	Radar	ComSat	Combined
Jan 21, 2021				
Belle Ile	9.0	6.2	10.9	**8.6**
Le Puy	6.0	8.0	2.7	**5.3**
Lyon	0.8	2.7	**1.7**	2.2
May 10 2021				
Belle Ile	0.6	1.2	0.4	**0.7**
Le Puy	56.5	68.4	45.0	**56.7**
Lyon	82.3	43.6	**59.6**	57.4

The results indicate that the combined estimation is closer to the ground truth measurements in most cases. It indicates that the measurements of the two methods are under- and overestimating at different circumstances, thus the combined method seems to *average* out these errors.

5 Discussion and Conclusions

The preliminary experiments demonstrate the superiority of merging rain estimates from communication satellites and weather radar data on the given test data. Not only are the spatial and temporal resolutions of the radar data increased but also the accuracy of measuring rain over longer time periods is improved. The authors believe that these encouraging results are due to the different acquisition techniques, e.g. ground-based and space-borne. The two data sources complement each other which leads to more accurate rain estimates compared to taking only one of the measurements alone. However, the proposed approach uses a fairly simple combination technique weighting both data sources in a fixed way.

Thus, in future work, we aim to investigate a dynamic weighting based on the confidence of the different methods. With changing weights temporally and per region the precipitation estimation could be even further improved. An additional research direction is using more advanced combination techniques or even end-to-end solutions based on machine learning techniques that take satellite terminal data and radar measurements as input.

6 Acknowledgments

This work has been supported by the Luxembourg National Research Fund (FNR) project MILAN, ref 14787240.

References

[1] R. J. Serafin, and J. W. Wilson. “Operational weather radar in the United States: Progress and opportunity,” *Bulletin of the American Meteorological Society*, **81**, 3, 2000, pp.501–518, doi:10.1175/1520-0477(2000)081<3C0501:OWRITU>3E2.3.CO;2.

[2] F. Giannetti, and R. Reggiannini. “Opportunistic Rain Rate Estimation from Measurements of Satellite Downlink Attenuation: A Survey.” *Sensors*, **21**, 17, 5872, 2021, doi: 10.3390/s21175872.

[3] F. Giannetti, M. Moretti, R. Reggiannini, and A. Vaccaro. “The NEFOCAST system for de-tection and estimation of rainfall fields by the opportunistic use of broadcast satellite signals,” *IEEE Aerospace and Electronic Systems Magazine*, **34**, 2019, pp.16—27, doi: 10.1109/MAES.2019.2916292.

[4] A. Gharanjik, M.B. Shankar, F. Zimmer, and B. Ottersten. “Centralized rainfall estimation using carrier to noise of satellite communication links,” *IEEE Journal on Selected Areas in Communications*, **36**, 5, 2018, pp.1065–1073, doi: 10.1109/JSAC.2018.2832798.

[5] K.V. Mishra, A. Gharanjik, M.B. Shankar, and B. Ottersten. “Deep learning framework for precipitation retrievals from communication satellites,” *In European Conference on Radar in Meteorology and Hydrology (ERAD)*, **7**, 2018.

[6] ITU. “Specific attenuation model for rain for use in prediction methods,” *ITU-R Recommendation P.838-3*, 2005.

[7] D.G. Krige. “A statistical approach to some basic mine valuation problems on the Witwatersrand,” *Journal of the Southern African Institute of Mining and Metallurgy*, **52**, 1951, pp.119-–139, doi: 10520/AJA0038223X_4792.

[8] S. Pulkkinen, D. Nerini, A. Perez Hortal, C. Velasco-Forero, U. Germann, A. Seed, and L. Foresti. “Pysteps: an open-source Python library for probabilistic precipitation nowcasting (v1.0),” *Geosci. Model Dev.*, **12**, 10, 2019, pp.4185—4219. doi: 10.5194/gmd-12-4185-2019.

[9] Available online: https://www.dwd.de/. Accessed 01.05.2022.

[10] Saltikoff, Elena and Haase, Günther and Delobbe, Laurent and Gaussiat, Nicolas and Martet, Maud and Idziorek, Daniel and Leijnse, Hidde and Novák, Petr and Lukach, Maryna and Stephan, Klaus. “OPERA the radar project,” *Atmosphere*, **10**, 6, 2019, p.320, doi: 10.3390/atmos10060320.

[11] Available online: https://donneespubliques.meteofrance.fr/. Accessed 01.05.2022.